Received August 31, 2017, accepted September 12, 2017, date of publication September 15, 2017, date of current version October 12, 2017.

Digital Object Identifier 10.1109/ACCESS.2017.2752804

A Precoding-Based Multicarrier Non-Orthogonal Multiple Access Scheme for 5G Cellular Networks

IMRAN BAIG, (Member, IEEE)
Department of Electrical and Computer Engineering, College of Engineering, Dhofar University, Salalah 211, Sultanate of Oman
e-mail: ibaig@du.edu.om

ABSTRACT Non-orthogonal multiple access (NOMA) has become one of the desirable schemes for the 5G cellular network standard due to its better cell coverage capability, higher data rate, and massive connectivity. Orthogonal frequency division multiplexing (OFDM) can be combined with NOMA to get the higher spectral efficiency. The main drawback of OFDM-based NOMA (OFDM-NOMA) scheme is high peak-to-average power ratio (PAPR). Therefore, this paper presents a new discrete-cosine transform matrix precoding-based uplink OFDM-NOMA scheme for PAPR reduction. Additionally, the proposed precoding-based uplink multicarrier NOMA scheme takes advantage of information spreading over the entire signal spectrum; thus, bit-error rate is also reduced. Simulation results show that the proposed precoding-based NOMA scheme outperforms as compared with the non-precoding-based NOMA schemes available in the literature.

INDEX TERMS NOMA, 5G cellular networks, PAPR, DCTM, BER.

I. INTRODUCTION

The Non-Orthogonal Multiple Access (NOMA) has become one of the desired candidates for the upcoming 5G Cellular Networks due to massive connectivity, higher data rate and low latency [1]–[6]. NOMA is a new signal design multiple access schemes where users will share time and frequency. Hence, more than one user can share the same frequency band simultaneously.

Orthogonal Frequency Division Multiplexing (OFDM) based NOMA is expected to provide the higher spectral efficiency, better cell coverage, massive connectivity and low latency. At the transmitter side, NOMA employs Superposition-Coding (SC) to send independent packets (signals) to several receivers simultaneously, and on the other hand, Successive-Interference-Cancellation (SIC) is employed to separate the signals of different users.

SIC is used at the cell center user (i.e., low power signal) to decode and cancel all the high power signals of paired users. SIC also introduce additional complexity and delay. Base on Shannon's theory, more complexity and delay will provide a better system. Direct demodulation will result in error propagation, and errors will occur in pairs in both signals.

If SIC is employed, there is sufficient CNR to decode the less robust signal, and the robust signal should have no error at all. So error propagation will not occur [7].

The requirements of mobile users are increasing day-by-day, and the industry is trying to satisfy all the demands. The researchers are trying to do their best to fulfill the customer demands. The old mobile communication standards like 1G, 2G, and 3G were focused on providing best voice services. When demand for data services increased the 3.5G (HSPA) and the 4G (LTE) was introduced, but still high data rate is required with the best quality of service. The upcoming new 5G mobile communication standard is expected to increase capacity 1000 times, i.e., connected devices per cell [8].

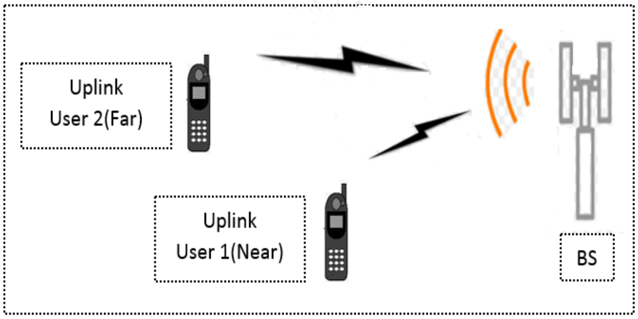

FIGURE 1. Uplink NOMA Architecture.

Fig. 1, illustrates the uplink NOMA scheme. This NOMA architecture is based on single cell scenario. The base station is communicating with two mobile users distributed geographically, i.e., *User 1*, which is near to the Base Station (BS)

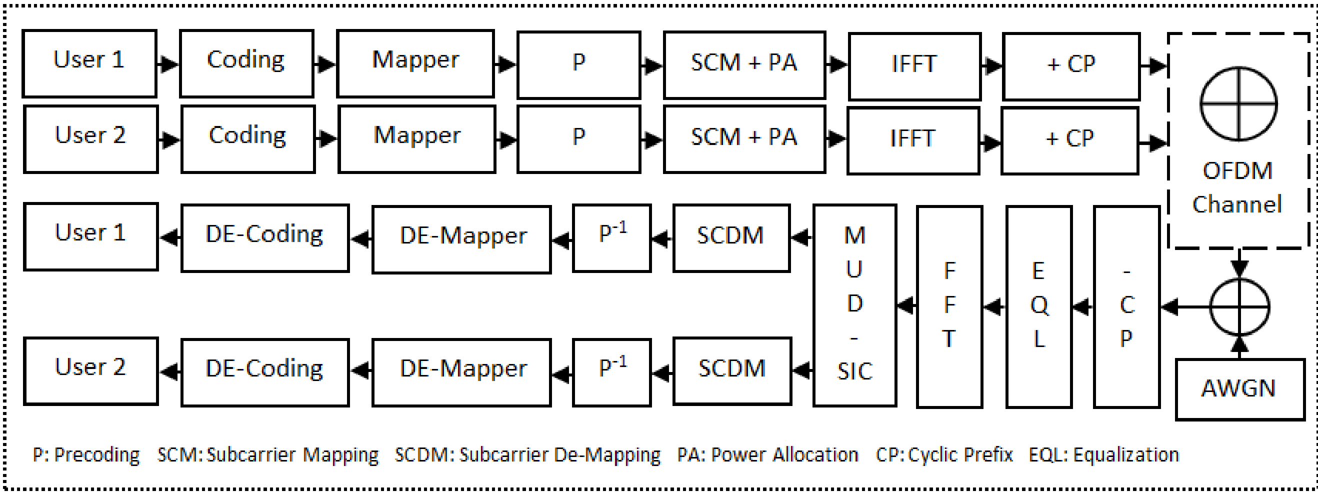

FIGURE 2. **A DCTM Precoding Based Uplink OFDM-NOMA System Model.**

and *User 2*, which is far from BS. NOMA can employ Orthogonal Frequency Division Multiple Access (OFDMA) to get the higher spectral efficiency.

Recently, a large number of different NOMA proposals can be seen in the literature for the upcoming 5G communication Networks. The Multicarrier NOMA schemes [9], [10] have got significant attention due to high spectral efficiency. These Multicarrier NOMA schemes support several users simultaneously by consuming the similar sub-carriers (sub-bands).

The uplink Multicarrier NOMA scheme proposed in [10] is more attractive and real, where authors proposed OFDM modulation without any use of coding or spreading. The Multi-User-Diversity (MUD) technique is employed at the receiver to separate the different users. Authors also limit the number of users under certain conditions to make system efficient.

Unfortunately, multicarrier NOMA has also some drawbacks. These weaknesses should be addressed carefully for its effective standardization. Among others, high Peak-to-Average Power Ratio (PAPR) problem is one of the main drawbacks. The PAPR problem makes OFDM based NOMA (OFDM-NOMA) scheme inefficient.

Many PAPR reduction schemes have been proposed in the literature. The signal independent linear precoding schemes [11]–[13] are more attractive due to simple linear implementations. Moreover, these systems do not need any side information or complex optimizations.

This paper is an extension of work done in [10]. A new precoding block has been added which is based on Discrete-Cosine Transform Matrix (DCTM) precoding. The DCTM precoder lowers the autocorrelation relationship among the modulated data and spread the information on each subcarrier equally. If the IFFT input (precoded modulated symbols) has low autocorrelation, then the in-phase additions will be less. Hence, PAPR is reduced. The information spreading by the DCTM precoder takes advantage of multipath fading channel and reduces the Bit-Error-Rate (BER).

This paper is structured as; Section II presents the proposed uplink Multicarrier NOMA scheme, Section III is based on computer simulations analysis, and the conclusion is presented in Section IV at the end.

II. PROPOSED SCHEME

Fig. 2, illustrates the proposed Discrete-Cosine Transform Matrix (DCTM) precoded uplink OFDM-NOMA scheme. For simplicity, a single cell set-up with two users have been considered, i.e., *User 1* and *User 2* distributed geographically under the same BS. Both users can communicate with the same BS using the same frequency subcarriers simultaneously.

The data is produced randomly for each user and then, modulated independently. After the modulation process, a DCTM precoding is applied to the constellation symbols. The precoding process lowers the autocorrelation relationship among the modulated data, then, sub-carrier mapping is accomplished in the localized mode like 4G LTE-A Cellular Network.

Before the IFFT, the power is allocated in the power domain to each user. At the receiver side, the different superimposed users are speared carefully by implementing MUD-SICs. Then, the inverse of DCT precoding matrix P^{-1} (since, $I = P.P^{-1}$) is applied to retrieve the estimated modulated data. This estimated modulated data is demodulated to get the estimated data (i.e., data transmitted by the different users, in our case *user 1* or *user 2*).

A. DCT AND DCTM

According to [14], the DCT can be written as: -

$$X_k = \Sigma_{n=0}^{N-1} x_n \cdot cos\left[\frac{\pi}{N}\left(n+\frac{1}{2}\right)k\right] \quad (1)$$

Kernel P of DCTM can be designed by the subsequent equation as below: -

$$P_{ij} = \begin{cases} \frac{1}{\sqrt{N}} i = 0, & 0 \leq j \leq N-1 \\ \sqrt{\frac{2}{N}} cos \frac{\pi(2j+1)j}{2N} & 1 \leq i \leq N-1 \\ & 0 \leq j \leq N-1 \end{cases} \quad (2)$$

and, the precoding matrix P can be written as: -

$$P = \frac{1}{\sqrt{N}} \begin{bmatrix} C_{00} & C_{01} & \dots & C_{0(L-1)} \\ C_{01} & C_{11}\dots & C_{1(L-1)} & \\ \vdots & \vdots & \ddots & \vdots \\ C_{(L-1)0} & C_{(L-1)1} & \dots & C_{(L-1)(L-1)} \end{bmatrix} \quad (3)$$

B. DCTM PRECODING BASED UPLINK OFDM-NOMA SCHEME

According to Fig. 2, the data is produced randomly/ independently and then, modulated by QPSK or M-QAM ($M = 16$ or 64). After the modulation process, precoding matrix P is applied to the Modulated Data D, and we get: -

$$Y_i = PD_i = [Y_0, Y_1, Y_2 \dots Y_{L-1}]^T \quad (4)$$

where, i denote the total number of users communicating simultaneously with the BS. After that, sub-carriers mapping is made in localized mode, then, transmit power PT_i is assigned in power domain for *the* i^{th} user based on the estimated distance between the BS and the resultant signal after the power allocation can be written as: -

$$\widehat{Y}_{i,l} = \sqrt{PT_i}\{Y_{i,l}\} \quad (5)$$

The complex precoding based Multicarrier NOMA baseband signal for the i^{th} user can be written as: -

$$x_n^{(i)} = \frac{1}{\sqrt{N}} \Sigma_{n=0}^{N-1} (\widehat{Y}_{i,l} \cdot e^{j2\pi \frac{k}{N} n}) \quad (6)$$

where $k = 0, 1, 2 \dots, N-1$. Complex precoding based uplink Multicarrier NOMA passband signal after Root-Raised Cosine (RRC) pulse shaping can be written as: -

$$x(t) = e^{j\omega_c t} \Sigma_{n=0}^{N-1} x_n^{(i)} \cdot r(t - n\check{T}) \quad (7)$$

where, $r(t)$ represents the baseband pulse, T is compressed symbol period after IFFT and ω_c indicate the carrier frequency. The pulse shaping (i.e., RRC) filter can be defined as: -

$$r(t) = \frac{sin\left(\frac{\pi t}{\check{T}}(1-\alpha)\right) + 4\alpha\frac{t}{\check{T}} \cdot cos\left(\frac{\pi t}{\check{T}}(1+\alpha)\right)}{\frac{\pi t}{\check{T}} \cdot \left(1 - \frac{16\alpha^2 t^2}{\check{T}^2}\right)}. \quad (8)$$

$0 \leq \alpha \leq 1$, α represent roll-off factor. The PAPR of precoded uplink OFDM-NOMA signal in (7) can be written as:-

$$PAPR = \frac{\max_{0 \leq t \leq N\check{T}} |x(t)|^2}{\frac{1}{N\check{T}} \int_0^{N\check{T}} |x(t)|^2 dt} \quad (9)$$

The precoding maintains the orthogonality of different symbols due to its cyclic auto-orthogonal property.

At the receiver side, after the equalization process, the MUD-SIC separate the signals of the different users. Then, sub-carrier de-mapping is performed in localized mode. After the sub-carrier de-mapping, the inverse P^{-1} of the DCT precoding matrix is applied to the received symbols of each user to remove the precoding effect (i.e., $I = P.P^{-1}$). The subsequent signal of the i^{th} user (*User 1* or *User 2*) can be written as:

$$Y_i = H_i P^{-1} X_i + N_i, \quad i = 1, 2, 3, \dots, k \quad (10)$$

C. THE EFFECT OF DCTM PRECODING

The precoding effect can analyze by generating modulated data of size 64. Aperiodic-Autocorrelation Function (ACF) is implemented to test the precoding performance. Fig. 3, illustrates the two different autocorrelation functions. The DCTM precoded sequences have low side-lobe values as compared to the non-precoded sequences side-lobe values. Low side-lobe values denote the low autocorrelation, and high side-lobe values indicate high autocorrelation. Low autocorrelation in the input of IFFT means rarer chances of in-phase additions at IFFT. Hence, PAPR is reduced. A detailed mathematical analysis of precoding effect on modulation symbols to reduce PAPR can be found in [15]. Hence, it is concluded that if the precoding is applied to the constellation symbols before the IFFT operations, a significant PAPR is reduced.

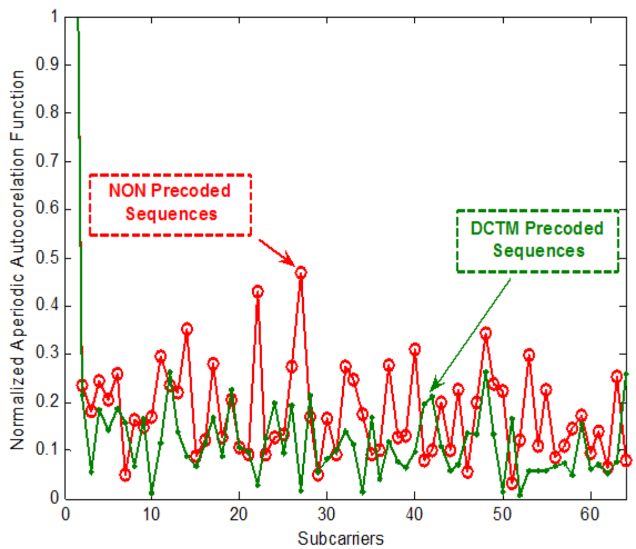

FIGURE 3. The Normalized Autocorrelation Function.

III. COMPUTER SIMULATIONS

This section presents a detailed computer simulation analysis of the proposed precoding based uplink OFDM-NOMA scheme. The data is generated randomly and independently, then, the produced data is modulated by employing any one of the modulation technique (i.e., QPSK or 16-QAM

TABLE 1. System parameters.

Number of Base Stations	1
Number of Users in Cell	2
Channel Bandwidth	5 MHz
Channel	ITU Pedestrian *A* channel
Oversampling Factor	8
User Sub-Carriers	16
System Sub-Carriers	512
Subcarrier Mapping Mode	Localized
Precoding	WHT and DCTM
Modulation	QPSK or 16-QAM or 64-QAM
Pulse Shaping	Root Raised Cosine (RRC)
RRC Roll-Off Factor	$\alpha = 0.22$
CCDF Clip Rate	10^{-3}
Equalization	MMSE

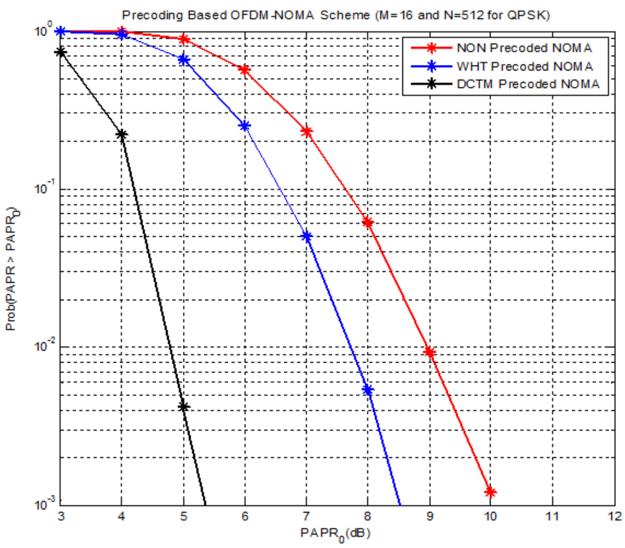

FIGURE 4. The Comparison between CCDF curves of PAPR using QPSK Modulation.

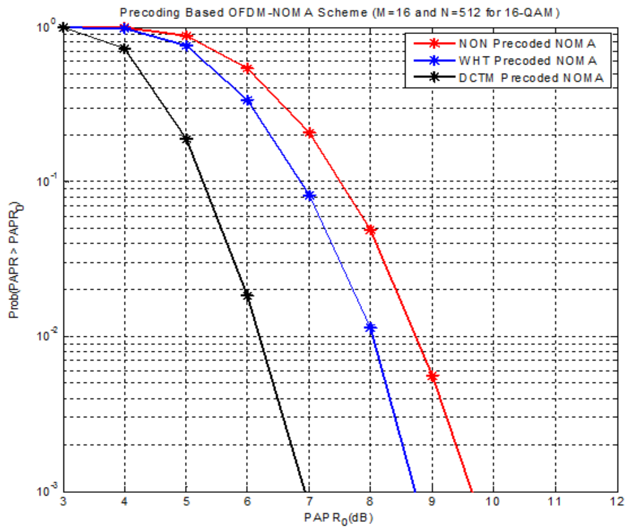

FIGURE 5. The Comparison between CCDF curves of PAPR using 16-QAM Modulation.

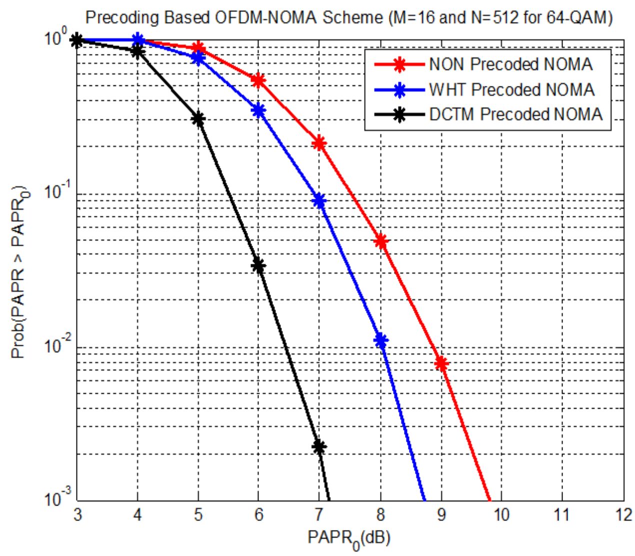

FIGURE 6. The Comparison between CCDF curves of PAPR using 64-QAM Modulation.

or 64-QAM). Table 1, show the different parameters used for the computer simulation to examine the proposed system.

Fig. 4, illustrates CCDF curves representing the PAPR for non-precoding based uplink Multicarrier NOMA scheme, WHT precoding based uplink Multicarrier NOMA scheme and DCTM precoding based uplink Multicarrier NOMA scheme, respectively, using QPSK modulation. At CCDF clip rate 10^{-3}, the PAPR of uplink Multicarrier NOMA signal without any precoding, WHT precoding based uplink Multicarrier NOMA signal and DCTM precoding based uplink Multicarrier NOMA signal is nearly 10.1 dB, 8.5 dB, and 5.4 dB, respectively.

Fig. 5, illustrates CCDF curves representing the PAPR for non-precoding based uplink Multicarrier NOMA scheme, WHT precoding based uplink Multicarrier NOMA scheme and DCTM precoding based uplink Multicarrier NOMA scheme, respectively, using 16-QAM modulation. At CCDF clip rate 10^{-3}, the PAPR of uplink Multicarrier NOMA signal without any precoding, WHT precoding based uplink Multicarrier NOMA signal and DCTM precoding based uplink Multicarrier NOMA signal is nearly 9.7dB, 8.7 dB, and 6.9 dB, respectively. Similarly, Fig. 6, illustrates CCDF curves representing the PAPR for non-precoding based uplink Multicarrier NOMA scheme, WHT precoding based uplink Multicarrier NOMA scheme and DCTM precoding based uplink Multicarrier NOMA scheme, respectively, using 64-QAM modulation. At CCDF clip rate 10^{-3}, the PAPR of uplink Multicarrier NOMA signal without any precoding, WHT precoding based uplink Multicarrier NOMA signal and DCTM precoding based uplink Multicarrier NOMA signal is nearly 9.8 dB, 8.8 dB, and 7.2 dB, respectively.

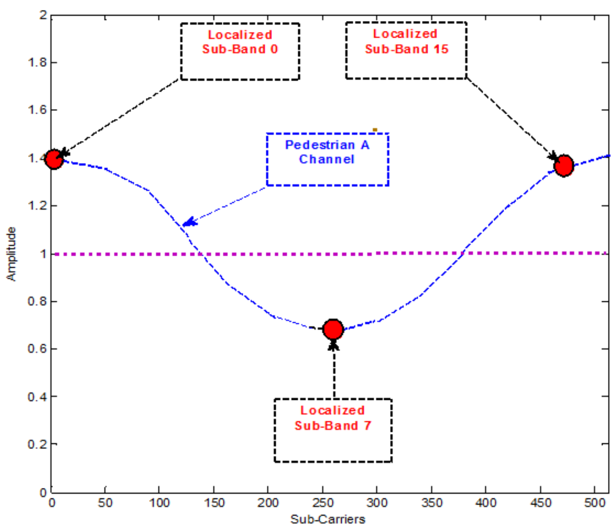

FIGURE 7. ITU Pedestrian *A* Channel Localized Sub-Carrier Design.

It is also observed that the PAPR of *User 1* and *User 2* is nearly the same because of power limitations of transmitter side set by the BS. Hence, the effect of power domain on the PAPR of the signal may be ignored.

Fig. 7, illustrates the position of different sub-bands for localized sub-carrier mapping mode in ITU pedestrian *A* channel.

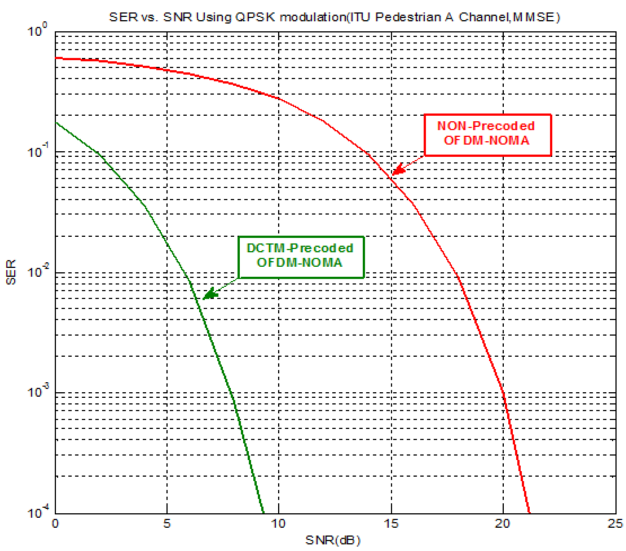

FIGURE 8. SER vs. SNR Comparison for sub-band 0 using QPSK modulation.

Fig. 8, illustrates SER vs. SNR analysis of the proposed scheme with the uplink Multicarrier NOMA scheme for sub-band 0. ITU pedestrian *an* outdoor channel is employed with the Additive White Gaussian Noise (AWGN), and MMSE equalization technique is used. It is evident from the Fig. 8 that the DCTM precoded uplink Multicarrier NOMA scheme shows significant SER gain over the non-precoded uplink

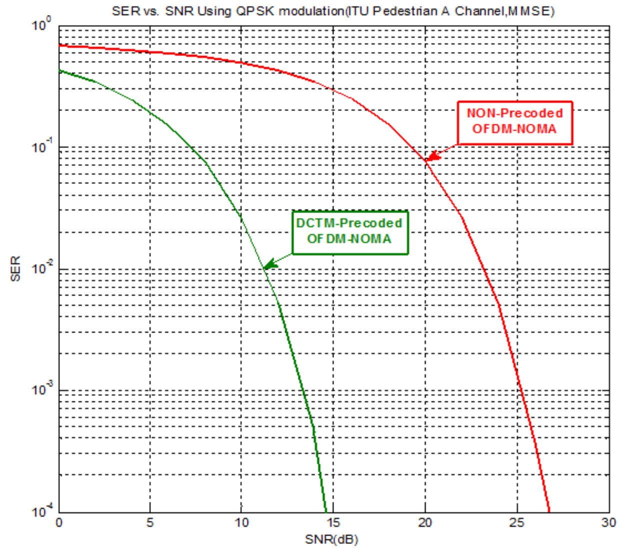

FIGURE 9. SER vs. SNR Comparison for sub-band 15 using QPSK modulation.

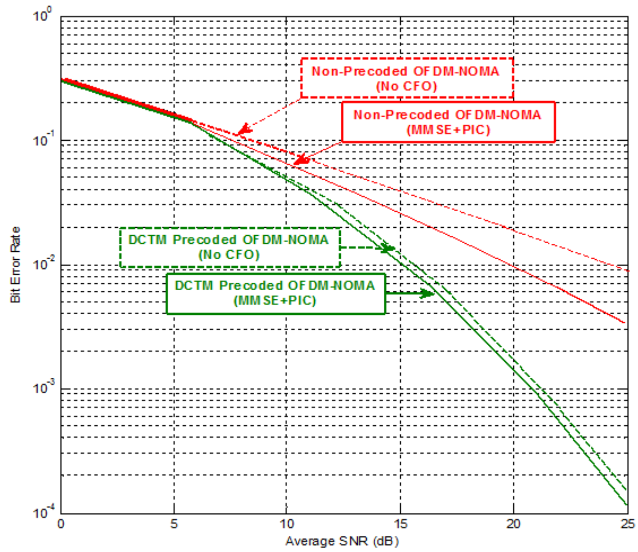

FIGURE 10. BER vs. SNR for DCTM precoded uplink OFDM-NOMA and non-precoded uplink OFDM-NOMA respectively, with random CFOs.

Multicarrier NOMA scheme available in the literature, for sub-band 0 by using QPSK modulation.

Fig. 9 illustrates SER vs. SNR analysis of the proposed scheme with the uplink OFDM-NOMA scheme for sub-band 15.

It is apparent from the Fig. 9 that the DCTM precoded uplink OFDM-NOMA scheme shows significant SER performance gain over the non-precoded uplink OFDM-NOMA scheme for sub-band 15 by using QPSK modulation. It is also noticed that the performance varies from 8 dB (i.e., sub-band 0) to 15 dB (i.e., sub-band 15) which is based on the spectrum chunk it occupies. In localized sub-band, SER vs. SNR performance is much better due to higher channel gain than average. On the other hand, according to the Fig. 7, the localized sub-band 15 has the lower channel gain, hence, performance gain is worse. Thus, localized mapping mode of sub-carriers lacks frequency diversity, and it should either use channel-dependent scheduling or sub-band hoping to handle this limitation.

Fig. 10, illustrates the BER vs. SNR performance analysis for the proposed precoding based uplink OFDM-NOMA scheme and non-precoded uplink OFDM-NOMA scheme respectively, using the random Carrier-Frequency-Offsets (CFOs). Minimum Mean Square Error (MMSE) is combined with Parallel Interference Cancellation (PIC) recently proposed in [16] is employed to evaluate the BER performance. Computer simulation shows that the PIC can remove the Multiple-Access-Interference (MAI) and provide good BER gain. The performance loss of the system is also acceptable when compared with the system without CFOs.

IV. CONCLUSION

In this paper, a precoding based uplink Multicarrier NOMA scheme has been presented and investigated through the computer simulations. Computer simulations demonstrate that the proposed precoding based scheme out-performs when compared with non-precoded schemes available in the literature. Proposed DCTM precoding based OFDM-NOMA scheme is signal independent; hence, no need of any side information. Therefore, it can be concluded that the proposed scheme may be one of the promising multiple access technique for the 5G Cellular Networks as compared to the other uplink Multicarrier NOMA schemes available in the literature.

REFERENCES

[1] Y. Saito, Y. Kishiyama, A. Benjebbour, T. Nakamura, A. Li, and K. Higuchi, "Non-orthogonal multiple access (NOMA) for cellular future radio access," in *Proc. IEEE 77th Veh. Technol. Conf. (VTC)*, Jun. 2013, pp. 1–5.

[2] L. Dai, B. Wang, Y. Yuan, S. Han, I. Chih-Lin, and Z. Wang, "Non-orthogonal multiple access for 5G: Solutions, challenges, opportunities, and future research trends," in *IEEE Commun. Mag.*, vol. 53, no. 9, pp. 74–81, Sep. 2015.

[3] H. Haci and H. Zhu, "Performance of non-orthogonal multiple access with a novel interference cancellation method," in *Proc. IEEE Int. Conf. Commun. (ICC)*, London, U.K., Jun. 2015, pp. 2912–2917.

[4] H. Haci, "Non-orthogonal multiple access (NOMA) with asynchronous interference cancellation," Ph.D. dissertation, Dept. Electron. Eng., Univ. Kent, Canterbury, U.K., 2015.

[5] J. Tong, L. Ping, and X. Ma, "Superposition coded modulation with peak-power limitation," *IEEE Trans. Inf. Theory*, vol. 55, no. 6, pp. 2562–2576, Jun. 2009.

[6] Z. Wei, J. Yuan, D. W. Ng, M. Elkashlan, and Z. Ding. (Sep. 2016). "A survey of downlink non-orthogonal multiple access for 5G wireless communication networks." [Online]. Available: https://arxiv.org/abs/1609.01856

[7] N. I. Miridakis and D. D. Vergados, "A survey on the successive interference cancellation performance for single-antenna and multiple-antenna OFDM systems," in *IEEE Commun. Surveys Tuts.*, vol. 15, no. 1, pp. 312–335, 1st Quart., 2013.

[8] J. Lee *et al.*, "LTE-advanced in 3GPP Rel-13/14: An evolution toward 5G," *IEEE Commun. Mag.*, vol. 54, no. 3, pp. 36–42, Mar. 2016, doi: 10.1109/MCOM.2016.7432169.

[9] Y. Tasi, G. Zhang, and X. Wang, "Orthogonal polyphase codes for constant envelope OFDM-CDMA system," in *Proc. IEEE WCNC*, Las Vegas, NV, USA, Apr. 2006, pp. 1396–1401.

[10] M. Al-Imari, P. Xiao, M. A. Imran, and R. Tafazolli, "Uplink non-orthogonal multiple access for 5G wireless networks," in *Proc. 11th Int. Symp. Wireless Commun. Syst. (ISWCS)*, Barcelona, Spain, 2014, pp. 781–785.

[11] K. Arsla and S. Soo Young, "Linear precoding techniques for OFDM-based NOMA over frequency-selective fading channels," *IETE J. Res.*, vol. 63, no. 4, pp. 536–551, 2017.

[12] I. Baig, N. ul Hasan, M. Zghaibeh, I. U. Khan, and A. S. Saand, "A DST precoding based uplink NOMA scheme for PAPR reduction in 5G wireless network," in *Proc. 7th Int. Conf. Modelling, Simulation, Appl. Optim. (ICMSAO)*, Sharjah, United Arab Emirates, 2017, pp. 1–4.

[13] A. Khan, M. B. Shahab, and S. Y. Shin, "PAPR reduction of uplink NOMA using Walsh Hadamard transform (WHT)," in *Proc. Korean Inst. Commun. Inf. Sci. Conf.*, 2016, pp. 413–414.

[14] N. Ahmed, T. Natarajan, and K. R. Rao, "Discrete cosine transform," *IEEE Trans. Comput.*, vol. C-23, no. 1, pp. 90–93, Jan. 1974.

[15] C. Tellambura, "Upper bound on peak factor of N-multiple carriers," *Electron. Lett.*, vol. 33, no. 19, pp. 1608–1609, Sep. 1997.

[16] F. S. Al-kamali, M. I. Dessouky, B. M. Sallam, F. Shawki, and F. E. Abd El-Samie, "Carrier frequency offset problem in DCT-SC-FDMA systems: Investigation and compensation," *ISRN Commun. Netw.*, vol. 2011, 2011, Art. no. 842093, doi: 10.5402/2011/842093.

IMRAN BAIG (M'15) received the M.Sc. degree in computer engineering from the University of Engineering Technology, Taxilla, Pakistan, in 2005 and the Ph.D. degree in electrical and electronic engineering from Universiti Teknologi PETRONAS, Malaysia, in 2012. He has been with the Department of Electrical and Computer Engineering, Dhofar University, Salalah, Oman, since 2015, where he is currently an Assistant Professor. He has authored and co-authored about 25 journal papers, one book chapter, and 14 conference papers; these papers have received over 200 citations. His research interests cover many aspects of the physical, medium access, and networking layers of wireless communications with a special emphasis on cellular radio networks, mobile ad hoc and sensor networks, and Internet security. He is a member of IET and the International Association of Engineers, Hong Kong. He was awarded as one of the Top 100 World's Best Scientists 2013 by IBC, Cambridge, U.K. His name is also included in the *Marquis Who's Who* booklet for years 2013, 2014, and 2015, respectively. He is an Editor-in-Chief of *ITEE Journal.* He has been also serving as a Designated Reviewer for many reputed journals of the IEEE, Elsevier, IET, and Springer.